PROCEEDINGS OF SCIENCE

Determination of $U_A(1)$ restoration from meson screening masses by using the entanglement PNJL model: Toward chiral regime

Masahiro Ishii*
Department of Physics, Graduate School of Sciences, Kyushu University, Fukuoka 812-8581, Japan
E-mail: ishii@phys.kyushu-u.ac.jp

Junichi Takahashi
Department of Physics, Graduate School of Sciences, Kyushu University, Fukuoka 812-8581, Japan
E-mail: takahashi@phys.kyushu-u.ac.jp

Hiroaki Kouno
Department of Physics, Saga University, Saga 840-8502, Japan
E-mail: kounoh@cc.saga-u.ac.jp

Masanobu Yahiro
Department of Physics, Graduate School of Sciences, Kyushu University, Fukuoka 812-8581, Japan
E-mail: yahiro@phys.kyushu-u.ac.jp

We determine temperature (T) dependence of $U_{\mathrm{A}}(1)$ restoration from meson screening masses calculated with 2+1 flavor lattice QCD, using Polyakov-loop extended Nambu–Jona-Lasinio (PNJL) model with entanglement vertex. The entanglement PNJL (EPNJL) model exhibits the $U_{\mathrm{A}}(1)$ anomaly through the Kobayashi–Maskawa–'t Hooft (KMT) interaction. T dependence of KMT interaction strength is determined from the difference between pion and a_0 meson screening masses. The strength is strongly suppressed around the pseudocritical temperature of chiral transition. Using this T-dependent KMT interaction, we draw the Columbia plot near the physical point. In the light-quark chiral-limit with the strange quark mass fixed at the physical value, the chiral transition becomes the second order. This indicates that there exists a tricritical point. Hence the location is estimated.

The 33rd International Symposium on Lattice Field Theory
14 -18 July 2015
Kobe International Conference Center, Kobe, Japan

*Speaker.

PoS(LATTICE 2015)201

1. Introduction

In the Quantum Chromodynamics (QCD) vacuum, $U_{\rm A}(1)$ symmetry is explicitly broken by the $U_{\rm A}(1)$ anomaly through the topologically nontrivial gauge configurations. For high temperature (T), the instanton density $dn_{\rm inst}(T)$ is suppressed by the Debye-type screening [1]:

$$dn_{\rm inst}(T) \sim dn_{\rm inst}(0)\exp\Big[-\pi^2\rho^2T^2\Big(\frac{2}{3}N_c+\frac{1}{3}N_f\Big)\Big], \tag{1.1}$$

where $N_c(N_f)$ means number of colors (flavors) and ρ means instanton radius. The suppresion suggests that $U_{\rm A}(1)$ symmetry is effectively restored at high temperature. The restoration of $U_{\rm A}(1)$ symmetry is related with the order of the chiral phase transition in 2-flavor QCD at zero light-quark mass. In Ref. [2], it is suggested that the order may be second order with 3d Izing $O(4)$ universality class if the effective restoration is not completed at $T = T_c$, where T_c is transition temperature for chiral phase transition. When $U_{\rm A}(1)$ symmetry is restored completely at $T = T_c$, the chiral transition becomes the first order [2]. Recently, however, it was pointed out in Ref. [3] that the second order is still possible. In this case, the universality class is not $O(4)$ but $U(2)_{\rm L}\times U(2)_{\rm R}$. There are many lattice QCD (LQCD) simulations and effective model analyses made so far to clarify the order and its universality class in the two-flavor chiral limit and the light-quark chiral limit where light-quark mass vanishes with strange-quark mass fixed at the physical value, but these are still controversial.

In this talk, we incorporate the effective restoration of $U_{\rm A}(1)$ symmetry in entantlement Polyakov-loop extended Nambu–Jona-Lasinio (EPNJL) model by introducing a temperature-dependent strength $K(T)$ to the Kobayashi-Maskawa-'t Hooft (KMT) determinant interaction. T dependence of $K(T)$ is well determined from the results of state-of-the-art 2+1-flavor lattice QCD simulations on pion and a_0-meson screening masses. Using the EPNJL model, we draw the Columbia plot near the physical point and determine the order of chiral transition in the light-quark chiral limit with m_s fixed at the physical value.

2. Model setting

2.1 EPNJL model

We start with the 2+1 flavor EPNJL model [4]. The Lagrangian density is

$$\begin{aligned}\mathscr{L} \;=\;& \bar\psi(i\gamma_\mu D^\mu-\hat m_0)\psi+G_{\rm s}(\Phi)\sum_{a=0}^{8}[(\bar\psi\lambda_a\psi)^2+(\bar\psi i\gamma_5\lambda_a\psi)^2]\\ &-\;K(T)\Big[\det_{f,f'}\bar\psi_f(1+\gamma_5)\psi_{f'}+\det_{f,f'}\bar\psi_f(1-\gamma_5)\psi_{f'}\Big]-\mathscr{U}(\Phi[A],\bar\Phi[A],T)\end{aligned} \tag{2.1}$$

with quark fields $\psi=(\psi_u,\psi_d,\psi_s)^T$ and $D^\mu=\partial^\mu+iA^\mu$ with $A^\mu=\delta^\mu_0 g(A^0)_a t_a/2=-\delta^\mu_0 ig(A_4)_a t_a/2$ for the gauge coupling g, where the λ_a (t_a) are the Gell-Mann matrices in flavor (color) space and $\lambda_0=\sqrt{2/3}\,\mathbf{I}$ for the unit matrix $\mathbf{I}$ in flavor space. The determinant in (2.1) is taken in flavor space. For the 2+1 flavor system, the current quark masses $\hat m_0={\rm diag}(m_u,m_d,m_s)$ satisfy a relation $m_s>m_l\equiv m_u=m_d$. In the EPNJL model, the coupling strength $G_{\rm s}(\Phi)$ of the scalar-type four-quark interaction depends on the Polyakov loop Φ and its Hermitian conjugate $\bar\Phi$ as

$$G_{\rm s}(\Phi)=G_{\rm s}(0)\times\left[1-\alpha_1\Phi\bar\Phi\right]. \tag{2.2}$$

This entanglement coupling is charge-conjugation and Z_3 symmetric.

For T dependence of $K(T)$, we assume the following form phenomenologically:

$$K(T) = \begin{cases} K(0) & (T < T_1) \\ K(0)e^{-(T-T_1)^2/b^2} & (T \geq T_1) \end{cases}. \tag{2.3}$$

For high T satisfying $T \gg T_1$, the form (2.3) is reduced to (1.1).

In the EPNJL model, the time component of A_μ is treated as a homogeneous and static background field, which is governed by the Polyakov-loop potential $\mathscr{U}$. In the Polyakov gauge, Φ and $\bar{\Phi}$ are obtained by

$$\Phi = \frac{1}{3}\mathrm{tr_c}(L), \qquad \bar{\Phi} = \frac{1}{3}\mathrm{tr_c}(L^*) \tag{2.4}$$

with $L = \exp[iA_4/T] = \exp[i\mathrm{diag}(A_4^{11}, A_4^{22}, A_4^{33})/T]$ for real variables A_4^{jj} satisfying $A_4^{11} + A_4^{22} + A_4^{33} = 0$. For zero chemical potential where $\Phi = \bar{\Phi}$, one can set $A_4^{33} = 0$ and determine the others as $A_4^{22} = -A_4^{11} = \cos^{-1}[(3\Phi - 1)/2]$.

We use the logarithm-type Polyakov-loop potential of Ref. [5] as $\mathscr{U}$, but we refit the parameter T_0 to 180 MeV in order to reproduce the chiral transition temperature $T_c = 154 \pm 9$ MeV [6, 7, 8] and deconfinement transition temperature $T_c^{\mathrm{deconf}} = 170 \pm 7$ MeV [9].

Making the mean field approximation (MFA) to (2.1) and the path integral over quark fields, one can get the thermodynamic potential (per unit volume) as

$$\Omega = U_\mathrm{M} + \mathscr{U} - 2\sum_{f=u,d,s}\int\frac{d^3\mathbf{p}}{(2\pi)^3}\Big[3E_{\mathbf{p},f} + \frac{1}{\beta}\ln\left[1 + 3(\Phi + \bar{\Phi}e^{-\beta E_{\mathbf{p},f}})e^{-\beta E_{\mathbf{p},f}} + e^{-3\beta E_{\mathbf{p},f}}\right]$$
$$+ \frac{1}{\beta}\ln\left[1 + 3(\bar{\Phi} + \Phi e^{-\beta E_{\mathbf{p},f}})e^{-\beta E_{\mathbf{p},f}} + e^{-3\beta E_{\mathbf{p},f}}\right]\Big] \tag{2.5}$$

with $\beta = 1/T$ and $E_{\mathbf{p},f} = \sqrt{\mathbf{p}^2 + M_f^2}$. The effective quark mass M_f is $M_f = m_f - 4G_\mathrm{s}(\Phi)\sigma_f + 2K(T)\sigma_{f'}\sigma_{f''}$ with $f \neq f' \neq f''$. The mesonic potential U_M is $U_\mathrm{M} = 2G_\mathrm{s}(\Phi)(\sigma_u^2 + \sigma_d^2 + \sigma_s^2) - 4K(T)\sigma_u\sigma_d\sigma_s$. Here, σ_f means the chiral condensate $\langle\bar{\psi}_f\psi_f\rangle$ for flavor f. We determine the mean-field variables ($X = \sigma_l, \sigma_s, \Phi, \bar{\Phi}$) from the stationary conditions:

$$\frac{\partial\Omega}{\partial X} = 0, \tag{2.6}$$

where isospin symmetry is assumed for the light-quark sector, i.e., $\sigma_l \equiv \sigma_u = \sigma_d$.

On the right-hand side of (2.5), the first term (vacuum term) in the momentum integral diverges. We then use the PV regularization [10]. In the scheme, the integral $I(M_f)$ is regularized as

$$I^{\mathrm{reg}}(M_f) = \sum_{\alpha=0}^{2} C_\alpha I(M_{f;\alpha}), \tag{2.7}$$

where $M_{f;0} = M_f$ and the $M_{f;\alpha}$ ($\alpha \geq 1$) mean masses of auxiliary particles. The parameters $M_{f;\alpha}$ and C_α should satisfy the condition $\sum_{\alpha=0}^{2} C_\alpha = \sum_{\alpha=0}^{2} C_\alpha M_{f;\alpha}^2 = 0$. We then assume $(C_0, C_1, C_2) = (1, 1, -2)$ and $(M_{f;1}^2, M_{f;2}^2) = (M_f^2 + 2\Lambda^2, M_f^2 + \Lambda^2)$. We keep the parameter Λ finite even after the subtraction (2.7), since the present model is non-renormalizable. The parameters are taken from Ref. [11] and they are $m_l = 6.2$ MeV, $m_s = 175.0$ MeV, $G_s(0)\Lambda^2 = 2.35$ and $K(0)\Lambda^5 = 27.8$ for $\Lambda = 795$ MeV. This parameter set reproduces mesonic observables at vacuum, i.e., the pion and kaon decay constants ($f_\pi = 92$ MeV and $f_K = 105$ MeV) and their masses ($M_\pi = 141$ MeV and $M_K = 512$ MeV) and the η'-meson mass ($M_{\eta'} = 920$ MeV). In the present work, we analyze LQCD results of Ref. [12] for pion and a_0-meson screening masses. In the LQCD simulation, the pion mass $M_\pi(0)$ at vacuum ($T = 0$) is 175 MeV and a bit heavier than the experimental value 138 MeV. We then change m_l to 9.9 MeV in the EPNJL model in order to reproduce $M_\pi(0) = 175$ MeV.

2.2 Meson screening mass

We derive the equations for pion and a_0-meson screening masses, following Ref [13, 14]. The current corresponding to a meson of type ξ is

$$J_\xi(x) = \bar{\psi}(x)\Gamma_\xi\psi(x) - \langle\bar{\psi}(x)\Gamma_\xi\psi(x)\rangle, \tag{2.8}$$

where $\Gamma_\pi = i\gamma_5\lambda_3$ for π meson and $\Gamma_{a_0} = \lambda_3$ for a_0 meson. We denote the Fourier transform of the mesonic correlation function $\eta_{\xi\xi}(x) \equiv \langle 0|\mathrm{T}\left(J_\xi(x)J_\xi^\dagger(0)\right)|0\rangle$ by $\chi_{\xi\xi}(q_0^2,\tilde{q}^2)$ as

$$\chi_{\xi\xi}(q_0^2,\tilde{q}^2) = i\int d^4x\, e^{iq\cdot x}\eta_{\xi\xi}(x), \tag{2.9}$$

where $\tilde{q} = \pm|\mathbf{q}|$ for $q = (q_0,\mathbf{q})$ and T stands for the time-ordered product. Using the random-phase (ring) approximation, one can obtain the Schwinger-Dyson equations for $\xi = \pi, a_0$ channels

$$\chi_{\xi\xi} = \frac{\Pi_\xi}{1 - 2G_\xi\Pi_\xi} \tag{2.10}$$

with the effective couplings G_π and G_{a_0} defined by

$$G_{a_0} = G_s(\Phi) + \frac{1}{2}K(T)\sigma_s,\ \ G_\pi = G_s(\Phi) - \frac{1}{2}K(T)\sigma_s, \tag{2.11}$$

and the one-loop polarization function Π_ξ defined by

$$\Pi_{a_0} = 4i[I_1 + I_2 - (q^2 - 4M^2)I_3],\ \ \Pi_\pi = 4i[I_1 + I_2 - q^2 I_3]. \tag{2.12}$$

M is the effective light-quark mass and $M = M_u = M_d$. At $T = 0$, three integrals I_1, I_2, I_3 are obtained by

$$\begin{aligned} I_1 &= \int\frac{d^4p}{(2\pi)^4}\mathrm{tr_c}\Big[\frac{1}{p'^2 - M}\Big],\ \ I_2 = \int\frac{d^4p}{(2\pi)^4}\mathrm{tr_c}\Big[\frac{1}{(p'+q)^2 - M^2}\Big], \\ I_3 &= \int\frac{d^4p}{(2\pi)^4}\mathrm{tr_c}\Big[\frac{1}{\{(p'+q)^2 - M^2\}(p'^2 - M^2)}\Big] \end{aligned} \tag{2.13}$$

with $p' = (p_0 + iA_4, \mathbf{p})$. $\mathrm{tr_c}$ means the trace in color space. For finite T, the corresponding equations are obtained by the replacement

$$p_0 \to i\omega_n = i(2n+1)\pi T,\ \ \int\frac{d^4p}{(2\pi)^4} \to iT\sum_{n=-\infty}^{\infty}\int\frac{d^3\mathbf{p}}{(2\pi)^3}. \tag{2.14}$$

Meson screening mass is defined by the exponential damping of the meson propagator $\eta_{\xi\xi}(r)$ in the long distance limit ($r \to \infty$):

$$M_{\xi,\mathrm{scr}} = -\lim_{r\to\infty} \frac{d\ln\eta_{\xi\xi}(r)}{dr}, \tag{2.15}$$

where $\eta_{\xi\xi}(r)$ is obtained by the Fourier transform of $\chi_{\xi\xi}(0,\tilde{q}^2)$ from the momentum $\tilde{q}$ space to the coordinate space r:

$$\eta_{\xi\xi}(r) = \frac{1}{4\pi^2 ir}\int_{-\infty}^{\infty} d\tilde{q}\ \tilde{q}\chi_{\xi\xi}(0,\tilde{q}^2)e^{i\tilde{q}r}. \tag{2.16}$$

It is not easy to make this Fourier transformation particularly at large r due to the highly oscilating function $e^{i\tilde{q}r}$. In order to avoid this problem, one can consider the Fourier transformation as a contour integral in the complex $\tilde{q}$ plane by using the Cauchy's integral theorem. However, it is reported in Ref. [15] that $\chi_{\xi\xi}(0,\tilde{q}^2)$ has logarithmic cuts in the vicinity of the real $\tilde{q}$ axis and heavy numerical calculations are necessary for evaluating the cut effects. In our previous work [14], we showed that these logarithmic cuts are unphysical and removable. If we make the **p** integral before taking the Matsubara summation $\sum_n$ in (2.14), we can express $I_3^{\mathrm{reg}}(0,\tilde{q}^2)$ as an infinite series of analytic functions:

$$I_3^{\mathrm{reg}}(0,\tilde{q}^2) = \frac{iT}{4\pi\tilde{q}}\sum_{j,n,\alpha} C_\alpha \sin^{-1}\left(\frac{\frac{\tilde{q}}{2}}{\sqrt{\frac{\tilde{q}^2}{4}+M_{j,n,\alpha}^2}}\right) \tag{2.17}$$

with

$$M_{j,n,\alpha}(T) = \sqrt{M_\alpha^2 + \{(2n+1)\pi T + A_4^{jj}\}^2}, \tag{2.18}$$

where $M_\alpha = M_{u;\alpha} = M_{d;\alpha}$. Each term of $I_3^{\mathrm{reg}}(0,\tilde{q}^2)$ has two physical cuts on the imaginary axis, one is an upward vertical line starting from $\tilde{q} = 2iM_{j,n,\alpha}$ and the other is a downward vertical line from $\tilde{q} = -2iM_{j,n,\alpha}$. There are two lowest branch points $\tilde{q} = 2iM_{j=1,n=0,\alpha=0} = 2iM_{j=2,n=-1,\alpha=0}$. We call them "threshold mass" in the sense that they come from the quark- antiquark continuum state.

We can obtain the meson screening mass $M_{\xi,\mathrm{scr}}$ as a pole of $\chi_{\xi\xi}(0,\tilde{q}^2)$,

$$\left[1-2G_\xi \Pi_\xi(0,\tilde{q}^2)\right]\big|_{\tilde{q}=iM_{\xi,\mathrm{scr}}} = 0. \tag{2.19}$$

If the pole at $\tilde{q} = iM_{\xi,\mathrm{scr}}$ is well isolated from the cut, i.e., $M_{\xi,\mathrm{scr}} < 2M_{j=1,n=0,\alpha=0}$, one can determine the screening mass from the pole location without making the $\tilde{q}$ integral.

3. Numerical Results

The EPNJL model has three adjustable parameters, α_1 in the entanglement coupling $G_{\mathrm{s}}(\Phi)$ and b and T_1 in the KMT interaction $K(T)$. These parameters can be clearly determined from 2+1 flavor LQCD data [12] for pion and a_0-meson screening masses, $M_{\pi,\mathrm{scr}}$ and $M_{a_0,\mathrm{scr}}$ as shown below.

Figure 1 shows T dependence of $M_{\pi,\mathrm{scr}}, M_{a_0,\mathrm{scr}}$. The EPNJL results for $M_{\pi,\mathrm{scr}}$ ($M_{a_0,\mathrm{scr}}$) are represented by solid (dotted) line and LQCD ones are plotted with closed squares (open circles). Best fitting is obtained, when $\alpha_1 = 1.0$, $T_1 = 0.79T_c = 121$ MeV and $b = 0.23T_c = 36$ MeV. The

PoS(LATTICE 2015)201

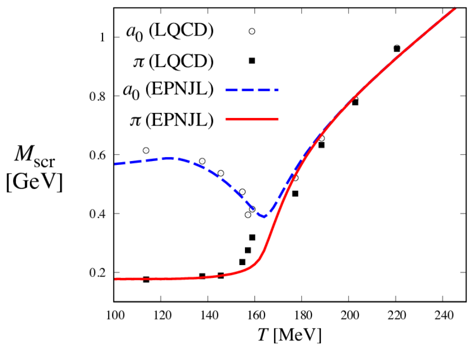

Fig. 1: T dependence of $M_{\pi,\rm scr}$ and $M_{a_0,\rm scr}$. The solid (dotted) line denotes $M_{\pi,\rm scr}$ ($M_{a_0,\rm scr}$) calculated by the EPNJL model. LQCD data are taken from Ref. [12]; closed squares (open circles) correspond to the 2+1 flavor data for $M_{\pi,\rm scr}$ ($M_{a_0,\rm scr}$). LQCD data are rescaled by the factor 154/196.

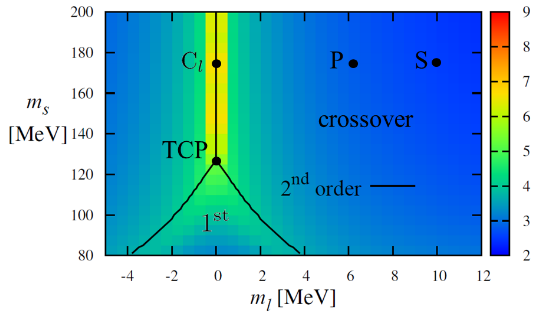

Fig. 2: Order of chiral transition near physical point in the m_l–m_s plane. The value of $\log[\chi_{ll}(T_c)]$ is shown by a change in hue. Simulation point, physical point, light-quark chiral-limit point and tricritical point are denoted by S, P, C_l and TCP. The solid lines stand for second-order chiral transitions.

parameters thus obtained lead to $K(T_c)/K(0) = 0.434$ and it indicates the rapid suppression of $K(T)$ in the vicinity of T_c, but $U_A(1)$ symmetry is not completely restored at T_c. Here, we rescale the LQCD results of [12] with multiplying them by the factor $154/196$ to reproduce $T_c = 154 \pm 9$ MeV. This is because T_c in the simulations [12] is about 196 MeV, although it becomes $T_c = 154 \pm 9$ MeV in finer LQCD simulations [6, 7, 8] close to the continuum limit.

Using the T-dependent KMT interaction, we draw the Columbia plot near the physical point in $m_l - m_s$ plane, as shown in Fig. 2. The S point represents the location of (m_l, m_s) for the LQCD simulation [12] and it is located at $(m_l, m_s) = (9.9\ [\text{MeV}], 175\ [\text{MeV}])$. S-point is close to light-quark chiral limit point (C_l), therefore, we can extrapolate the LQCD results [12] from S-point to C_l-point by using the EPNJL model. Varying both m_l and m_s, we determine the order of chiral transition from the divergence of T dependence of chiral susceptibility $\chi_{ll}(T)$ and the discontinuity of chiral condensate. The value of $\log[\chi_{ll}(T_c)]$ is denoted by a change in hue. In the light-quark chiral-limit with the strange quark mass (m_s) fixed at the physical value $m_s = m_s^{\rm phys} = 175$ MeV, the chiral transition becomes the second order in the mean field approximation. The second-order chiral transitions (solid lines) meet at $(m_l^{\rm tric}, m_s^{\rm tric}) \approx (0, 0.726 m_s^{\rm phys}) = (0[\text{MeV}], 127[\text{MeV}])$. This is a tricritical point (TCP) of chiral phase transition.

4. Summary

In summary, we incorporated the effective restoration of $U_A(1)$ symmetry in the 2+1 flavor EPNJL model by introducing a T-dependent coupling strength $K(T)$ to the KMT interaction. The T dependence was well determined from state-of-the-art 2+1 flavor LQCD data on pion and a_0-meson screening masses. The strength $K(T)$ thus obtained is suppressed in the vicinity of the pseudocritical temperature of chiral transition. However, $U_{\rm A}(1)$ symmetry breaking still remains at T_c. Using the EPNJL model with the present parameter set, we showed that, at least in the mean field level, the order of chiral transition is second order at the light-quark chiral-limit point of $m_l = 0$ and $m_s = 175$ MeV (the physical value). This result indicates that there exists a tricritical point near the light-quark chiral-limit point in the m_l–m_s plane. We then estimated the location of the tricritical point as $(m_l^{\rm tric}, m_s^{\rm tric}) \approx (0, 0.726 m_s^{\rm phys}) = (0[\rm MeV], 127[\rm MeV])$.

Acknowledgments

M. I, J. T., H. K., and M. Y. are supported by Grant-in-Aid for Scientific Research (No. 27-3944, No. 25-3944, No. 26400279 and No. 26400278) from the Japan Society for the Promotion of Science (JSPS).

References

[1] R. D. Pisarski, and L. G. Yaffe, Phys. Lett. B **97**,

[2] R. D. Pisarski, and F. Wilczek, Phys. Rev. D **29**, 338(R) (1984). 110 (1980).

[3] A. Pelissetto, and E. Vicari, Phys. Rev. D **88**, 105018 (2013).

[4] T. Sasaki, Y. Sakai, H. Kouno, and M. Yahiro, Phys. Rev. D **84**, 091901(R) (2011).

[5] S. Rößner, C. Ratti, and W. Weise, Phys. Rev. D **75**, 034007 (2007).

[6] S. Borsanyi *et al.*, J. High Energy Phys. 09 (2010) 073.

[7] A. Bazavov, T. Bhattacharya, M. Cheng, C. DeTar, H. -T. Ding, S. Gottlieb, R. Gupta, and P. Hegde *et al.*, Phys. Rev. D **85**, 054503 (2012).

[8] K. Kanaya, [arXiv: 1012.4235]; [arXiv: 1012.4247].

[9] Y. Aoki, S. Borsányi, S. Dürr, Z. Fodor, S. D. Katz, S. Krieg, and K. K. Szabo, J. High Energy Phys. 06 (2009) 088 [arXiv:0903.4155].

[10] W. Pauli, and F. Villars, Rev. Mod. Phys. **21**, 434 (1949).

[11] V. Bernard, and D. Vautherin, Phys. Rev. D **40**, 1615 (1989).

[12] M. Cheng, S. Datta, A. Francis, J. van der Heide, C. Jung, O. Kaczmarek, F. Karsch, and E. Laermann *et al.*, Eur. Rhys. J. C **71**, 1564 (2011).

[13] S. P. Klevansky Rev. Mod. Phys. **64**, 649 (1992); T. Hatsuda, and T. Kunihiro Phys. Rep. **247**, 221 (1994); M. Buballa Phys. Rep. **407**, 205 (2005).

[14] M. Ishii, T. Sasaki, K. Kashiwa, H. Kouno, and M. Yahiro, Phys. Rev. D **89**, 071901(R) (2014).

[15] W. Florkowski, Acta Phys. Pol. B **28**, 2079 (1997) .